Journal of Mechanics in Medicine and Biology

MATHEMATICAL MODELING OF THE INTERPLAY BETWEEN STRESS AND ANISOTROPIC GROWTH OF AVASCULAR TUMORS

FERNANDO VALDÉS-RAVELO
Centro de Inmunología Molecular
Playa, Havana 11600, Cuba.
fernandov@cim.sld.cu

ARIEL RAMÍREZ-TORRES
Instituto de Investigaciones en Matemáticas Aplicadas y en Sistemas,
Universidad Nacional Autónoma de México
Apartado Postal 20-126, 01000 CDMX, México
ariel.ramirez@iimas.unam.mx

Dipartimento di Scienze Mathematiche
"G. L. Lagrange", Politecnico di Torino, Torino 10129, Italia
torres@calvino.polito.it

REINALDO RODRÍGUEZ-RAMOS[†], JULIÁN BRAVO-CASTILLERO[‡], RAÚL GUINOVART-DÍAZ[§]
Departamento de Matemáticas, Facultad de Matemática y Computación,
Universidad de La Habana
Vedado 10400, La Habana, Cuba
[†]*reinaldo@matcom.uh.cu,* [‡]*jbravo@matcom.uh.cu,* [§]*guino@matcom.uh.cu*

JOSÉ MERODIO[□], RAIMONDO PENTA[■]
[□]*Departamento de Mecánica de los Medios Continuos y T. Estructuras, E.T.S. de Caminos, Canales y Puertos,*
Universidad Politécnica de Madrid
Madrid 28040, España
jose.merodio@upm.es

[■]*School of Mathematics and Statistics, Mathematics and Statistics Building*
University of Glasgow, University Place Glasgow G12 8SQ, UK
Raimondo.Penta@glasgow.ac.uk

AURA CONCI
Instituto de Computación, Universidade Federal Fluminense
Río de Janeiro 24210-346, Brasil
aconci@ic.uff.br

FEDERICO J. SABINA[°], CATHERINE GARCÍA-REIMBERT[•]
Instituto de Investigaciones en Matemáticas Aplicadas y en Sistemas,
Universidad Nacional Autónoma de México
Apartado Postal 20-126, 01000 CDMX, México
[°]*fjs@mym.iimas.unam.mx,* [•]*cgr@mym.iimas.unam.mx*

In this work we propose a new mathematical framework for the study of the mutual interplay between anisotropic growth and stresses of an avascular tumor surrounded by an external medium. The mechanical response of the tumor is dictated by anisotropic growth, and reduces to that of an elastic, isotropic, and incompressible material when the latter is not taking place. Both proliferation and death of tumor cells are

in turn assumed to depend on the stresses. We perform a parametric analysis in terms of key parameters representing growth anisotropy and the influence of stresses on tumor growth in order to determine how these effects affect tumor progression. We observe that tumor progression is enhanced when anisotropic growth is considered, and that mechanical stresses play a major role in limiting tumor growth.

Keywords: Avascular tumor; Linear elasticity; Anisotropic growth; Stress-driven growth.

1. Introduction

Cancer has become a leading cause of death by disease in many countries [1] because of its poor prognosis and high rate of incidence. It is caused by mutations in a normal cell, which induce an uncontrolled proliferation. Cancer evolution is extremely complex; however some features in its progression can be associated with the generation and accumulation of mechanical stresses. In fact, it is widely accepted that mechanical stress is one of the key factors regulating cell growth and death [19;20;27;45]. It is well-known that healthy cells possess specific mechanisms to maintain an ideal stress state [3], corresponding to stress conditions maintained in tissue homeostasis. The genesis of a tumor could be seen either as a failure of such mechanisms (so that the cells are unable to return to their initial stress state), or as an alteration of the information of stress conditions during homeostasis, such that the cell self-regulates to an aberrant stress condition. According to Ambrosi et al. (2012) [3], a possible anti-cancer strategy could reside in forcing the cells to come back to their mechanically ideal stress state. Thus, the understanding of stress development in the tumor is of major importance.

Mathematical models are useful in order to understand cancer behavior, and formulate predictions to support the design of anti-cancer therapies. There have been several investigations on the subject with different approaches including continuum and discrete representations of cancer. Several models range from cellular automata to compact cellular spheroids; from assuming that tumors maintain their solid shape to model the cell adhesion using, in some of them, elasticity theory and in the others different physical principles, creating a wide variety of methods [2;9;22]. Drasdo and Hohme (2005) [13] and Carmenate et al. (2013) [10] deal with the cell level. In these models the tumor geometry is set aside and generally describes system dynamics of various cell populations. Others works focus on the macroscopic scale using a mechanical approach. For instance, Araujo and McElwain (2005b) [8], Jones et al. (2000) [21] and Ngwa and Agyingi (2012) [28] assume a constitutive equation from linear elasticity theory in order to relate growth with deformation. Moreover, discrete cell based approaches have been also considered [4;46], as well as multiscale models based on homogenization techniques, such as Penta et al. (2014) [32] and Penta et al. (2017) [33] for avascular tumor growth and vascular tumor mechanics, respectively. The latter models have the potential to incorporate details of the tumor microstructure, and they have only recently been investigated from a practical viewpoint due to their computational complexity (see, e.g. the works of Penta and Ambrosi (2015) [30] and Mascheroni et al. (2017) [25] based on the theoretical framework developed for rigid vascular tumors in Shipley et al. (2010) [40] and Penta et al. (2015) [31], respectively).

In the present work, a macroscopic approach is used for studying the avascular stage of a solid tumor and the proposed model represents an extension of that proposed by Ngwa and Agyingi (2012) [28], where the authors modeled the evolution of growth-induced stress in a spherical tumor surrounded by an external medium and exhibiting isotropic properties. Here we generalize the model in Ngwa and Agyingi (2012) [28] by considering a constitutive relationship which accounts for anisotropic growth as done in Araujo and McElwain (2005b) [8] and relating cell proliferation

and death to the stress, thus accounting for stress-dependent growth. The effect of the parameters representing growth anisotropy and the influence of stress on tumor progression is explored via a parametric analysis.

2. Tumor Model

In this section, we present the mathematical model in detail, which reads as a generalization of the study by Ngwa and Agyingi (2012) [28], we embrace the following set of assumptions.

i) The population of healthy and malignant cells form a single population, which is considered a continuum.
ii) There is adhesion among living tumor cells at the boundary, which holds the tumor in a solid state and balances the expansive force caused by the internal cell proliferation.
iii) The tumor is represented as a sphere and spherical symmetry is maintained at all times.
iv) There is a constant nutrient concentration in the tumor boundary.
v) The tumor is in a state of diffusive equilibrium. Moreover, nutrient consumption rate is proportional to nutrient concentration and tumor cell density.
vi) cell proliferation rate is proportional to nutrient concentration and tumor cell density, while cell death is proportional to the cell density. But in the presence of stresses, cell proliferation is inhibited and cell death is promoted.
vii) The tumor is considered an isotropic and incompressible elastic material.
viii) The tumor is surrounded by an external medium, which is likewise modeled as an incompressible and isotropic elastic material.

The first three assumptions represent a substantial simplification of the tumor growth process. The first one is embraced to avoid the structural and mechanical difference between different kind of cells. In general, there exist several types of cells in the tumor interior which are not necessarily malignant, such as endothelial cells [24], and those belonging to the immunological system [29;17]. Moreover, tumor cells can exhibit differences from both the metabolic (necrotic, hypoxic and proliferating cells [44]) and genetic (different tumoral clones, heterogeneous tumor [5;26]) points of view. The second assumption guarantees that the tumor maintains a solid shape with a well delimited boundary, which is fairly reasonable when considering the case for avascular solid tumors. Assumption iii) is a simplification of the geometry, which is commonly adopted to simplify the mathematical formulation [2;21;28;34], however in Helmlinger et al. (1997) [19], it is shown that tumors growing in free suspension adopt a spherical shape, while those growing within an agarose gel take an ellipsoidal geometry due to anisotropic stresses. Moreover, in the avascular stage, the tumor has availability of nutrients and occupies very little space, so that its conditions are similar to the ones depicted in Helmlinger's experiments [19] and it is therefore reasonable to assume spherical symmetry. Because of the wide nutrient disposition, the concentration of nutrients in the tumor is limited only by its diffusion velocity and not by the concentration at the tumor boundary. Thus, hypothesis iv) is just a mathematical simplification, but not from the modeling point of view. The remaining four assumptions have technical implications which are dealt with in the remainder of this section.

Hereinafter, the following notation is used:

Variable	**Definition**

t	Time
r	Radial coordinate
$R(t)$	Radius of the tumor at time t
R_0	Radius of the tumor at $t = 0$
$c(r,t)$	Nutrient concentration inside the tumor
c_b	Nutrient concentration at the boundary
$\mathbf{u}(r,t)$	Tumor cell displacement
$\boldsymbol{v}(r,t)$	Tumor cell displacement velocity
$\boldsymbol{\sigma}$	Cauchy stress tensor of the tumor
$\boldsymbol{\sigma^e}$	Cauchy stress tensor of the external medium
$\boldsymbol{e}$	Strain tensor of the tumor
$\boldsymbol{e^e}$	Strain tensor of the external medium
ρ	Tumor cell density

Table 1: Model variable definitions

2.1. *Kinematics and equilibrium equations*

The equation describing the motion of a surface $S = 0$ is

$$\frac{DS}{Dt} = 0, \tag{1}$$

where

$$\frac{D}{Dt} \equiv \frac{\partial}{\partial t} + \boldsymbol{v} \cdot \nabla$$

is the material derivative. Because of the radial symmetry, the material surface of the tumor is given by $S = r - R(t)$ and the velocity field has the form $\boldsymbol{v} = (v_r, 0, 0)$, leading to

$$\frac{dR}{dt} = v_r(R,t). \tag{3}$$

The above equation models the growth rate of the tumor. Now, from hypothesis i), the tumor is considered a continuum and the forces per unit area can be represented by the Cauchy stress tensor $\boldsymbol{\sigma}$. Particularly, inertial factors are neglected due to the cells low velocities, and body forces are ignored. In fact, according to Hemlinger's experiments, gravity does not play a major role [3]. Hence, assuming that no other volume forces are being exerted on the tumor mass, only contact forces are relevant and the equilibrium equation simply reads:

$$\nabla \cdot \boldsymbol{\sigma} = 0. \tag{4}$$

Since radial symmetry is considered and $\boldsymbol{\sigma} = \text{diag}\{\sigma_r, \sigma_\theta, \sigma_\phi\}$, the only relevant component of equation (4) is

$$\frac{\partial \sigma_r}{\partial r} + \frac{2}{r}(\sigma_r - \sigma_\theta) = 0, \tag{5}$$

bearing in mind that $\sigma_\theta = \sigma_\phi$.

2.2. *Constitutive equation*

In modeling some problems related to solids, one of the most important questions is how to choose the constitutive law, which relates the stress σ_{ij} with the material strain e_{ij}. According to Araujo and McElwain (2005b) [8], linear elasticity models which just consider isotropic growth are insufficient to describe the stress evolution in a growing tissue, because they do not reflect the stress relaxation effect, which is characteristic of viscoelastic materials. For example in a non-linear framework, in Ramírez-Torres et al. (2015) [34] and Ramírez-Torres et al. (2017) [35] is considered an anisotropic form for the growth tensor. In particular, this assumption leads to different patterns in tumor growth and solid stresses in agreement with experimental studies. On the other hand, purely elastic materials do not change their internal structure to adapt to the new stress conditions, but there are ways to obtain the effect of stress relaxation in a linear elastic model (see e.g., the work on anisotropic growth by Araujo and McElwain (2005b) [8]). Although deformations remain small, the linear elasticity theory offers acceptable results, reflecting the qualitative tissue behavior [18;39]. In the present work, is considered a constitutive law where the deformation due to elastic response of the material takes place in a linear fashion, but the deformation due to the growth is limited, since elastic materials can not deform indefinitely. Thus, locally the elastic response is linear with respect to the change in strain but globally is nonlinear because of the convective effects. That is to say, the nonlinearity is obtained by considering the dependence of r with respect to t in the time derivative. Hence, the law could be used for large displacements [21]. Following the ideas proposed in Araujo and McElwain (2005) [8] and Jones et al. (2000) [21], it yields

$$e_{ij} := \frac{1}{2}\left(\nabla \mathbf{u} + (\nabla \mathbf{u})^T\right)_{ij} = g\gamma_\theta \mathbf{e}_i \otimes \mathbf{e}_i + g\left(\gamma_r - \gamma_\theta\right)\mathbf{e}_r \otimes \mathbf{e}_r + \frac{1}{2E}(3\sigma_{ij} - \delta_{ij}\sigma_{kk}) \tag{6}$$

where $i, j, k = r, \theta, \phi$, E is Young's modulus, $g = g(r, t)$ is the growth factor (represents the tumor volumetric growth rate), $\mathbf{e}_i$ is the orthonormal basis in spherical coordinates, $\gamma_r, \gamma_\theta \in \mathbb{R}_+$ represent the tumor growth anisotropy terms in the radial and transversal directions respectively with (see Araujo and McElwain (2005) [8])

$$\gamma_r + 2\gamma_\theta = 1. \tag{7}$$

For $\gamma_r \equiv \gamma_\theta \equiv 1/3$, the constitutive equation from Jones et al. (2000) [21] and Ngwa and Agyingi (2012) [28], is obtained. Here, we generalize the latter work to anisotropic growth. On the other hand, if $g \equiv 0$ in (6) we get Hooke's law of an incompressible material. Because of hypothesis vii), the Poisson ratio ν is set to 0.5.

As mentioned in Araujo and McElwain (2004) [6] and Cheng et al. (2009) [12], growth is expected to be further enhanced along the directions of minimum compressive stresses. Although there are no experimental data at hand, the function γ_θ, which is assumed to depend on the stress difference

$$\beta = \sigma_r - \sigma_\theta, \tag{8}$$

should fulfill the properties given in Table 2.

Constraint	**Description**
$0 \leq \gamma_\theta(\beta) \leq 1/2$	γ_θ is relative growth in transversal directions.
$\gamma_\theta(0) = 1/3$	Isotropic growth when $\beta \equiv 0$.
$\gamma_\theta(\beta + x) \leq \gamma_\theta(\beta) \Leftrightarrow x \leq 0$	γ_θ decreases with respect to β.

$\lim_{\beta\to+\infty}\gamma_\theta(\beta)=0$	If $\beta \gg 1N/cm^2$, there is almost no growth in the transversal direction.
$\lim_{\beta\to-\infty}\gamma_\theta(\beta)=1/2$	If $\beta \ll -1N/cm^2$, there is almost no growth in the radial direction.

Table 2: Necessary properties for the function γ_θ.

Thus, the following law, which satisfies the constraints given in Table 2, is proposed

$$\gamma_\theta = \frac{1}{e^{a\beta}+2}, \tag{9}$$

where a is a positive physical quantity corresponding to the inverse of the stress dimension. Furthermore, γ_r is defined using the constraint (7), that is $\gamma_r = 1-2\gamma_\theta$.

It should be noted that the proposed constitutive relation must be invariant with respect to the reference system [21]. For this purpose, as in Jones et al. (2000) [21] and Ngwa and Agyingi (2012) [28], the Jaumann derivative is applied to (6) (the Jaumann derivative is a material derivative in a frame that rotates with the local angular velocity of the medium). Then, from (6),

$$\begin{aligned}\frac{1}{2}\left(\nabla\boldsymbol{v}+(\nabla\boldsymbol{v})^T\right) = {}& \frac{Dg}{Dt}(\gamma_\theta \mathbf{e}_i\otimes\mathbf{e}_i+(\gamma_r-\gamma_\theta)\,\mathbf{e}_r\otimes\mathbf{e}_r)\\ &+ g\left(\frac{D\gamma_\theta}{Dt}\mathbf{e}_i\otimes\mathbf{e}_i+\frac{D(\gamma_r-\gamma_\theta)}{Dt}\mathbf{e}_r\otimes\mathbf{e}_r\right)+\frac{1}{2E}\frac{D}{Dt}\left(3\sigma-\mathrm{tr}(\sigma)\mathbf{I}\right),\end{aligned}$$

where $\mathrm{tr}(\sigma)$ denotes the trace operator of σ and $\mathbf{I}$ is the identity tensor.

Using (7), the trace of the constitutive relation (10) leads to

$$\frac{Dg}{Dt} = \nabla\cdot\boldsymbol{v}. \tag{10}$$

Upon substitution of this result into (10), the constitutive law reads

$$\begin{aligned}\frac{1}{2}\left(\nabla\boldsymbol{v}+(\nabla\boldsymbol{v})^T\right) = {}& (\nabla\cdot\boldsymbol{v})(\gamma_\theta \mathbf{e}_i\otimes\mathbf{e}_i+(\gamma_r-\gamma_\theta)\,\mathbf{e}_r\otimes\mathbf{e}_r)\\ &+ g\left(\frac{D\gamma_\theta}{Dt}\mathbf{e}_i\otimes\mathbf{e}_i+\frac{D(\gamma_r-\gamma_\theta)}{Dt}\mathbf{e}_r\otimes\mathbf{e}_r\right)+\frac{1}{2E}\frac{D}{Dt}\left(3\sigma-\mathrm{tr}(\sigma)\mathbf{I}\right).\end{aligned} \tag{11}$$

2.3. *External medium*

Because of assumption viii), the external medium satisfies Hooke's law of an incompressible material,

$$\sigma^e_{ij} = -p\delta_{ij}+\frac{2E}{3}e^e_{ij}, \tag{12}$$

where $-p$ can be identified with isotropic pressure. Without loss of generality it is assumed that $\lim_{r\to\infty} p(r,t)=0$, then $\sigma^e_{ij}=0$ when $r\to\infty$ [28]. In particular, the radial stress σ_r and the displacement u_i are supposed continuous at the tumor boundary $r=R$.

2.4. *Growth equation*

For a living tissue, growth can be interpreted as the difference between cell production and cell death. Ignoring mechanical effects, using the mass conservation continuity equation and hypothesis vi), we can write

$$\underbrace{\frac{\partial \rho}{\partial t} + \nabla \cdot (\boldsymbol{v}\rho)}_{growth} = \underbrace{\alpha c \rho}_{cell\ proliferation} - \underbrace{k\rho}_{cell\ death}, \tag{13}$$

where α and k are positive numbers, which represent proliferation and death rates, respectively.

As was mentioned in the introduction, from a mechanical point of view, the stress plays an important role in the regulation of cell proliferation and death. However, as result of the external tissue displacement, the stress is accumulated while the tumor keeps growing and it could possibly delay or even stop its growth. Then, the following alternative equation to (13) is considered

$$\underbrace{\frac{\partial \rho}{\partial t} + \nabla \cdot (\boldsymbol{v}\rho)}_{growth} = \underbrace{\alpha c \rho (1 - \eta_1 \sqrt{\boldsymbol{\sigma}:\boldsymbol{\sigma}})}_{cell\ proliferation} - \underbrace{k\rho(1 + \eta_2 \sqrt{\boldsymbol{\sigma}:\boldsymbol{\sigma}})}_{cell\ death}, \tag{14}$$

where $\eta_1, \eta_2 \in \mathbb{R}_+$ are constants representing the dependency of cell proliferation and death on stress. The minus sign in the first term of the right-hand-side of (14) means that cell division is inhibited by the presence of stress, whereas the plus sign in the second term of the right-hand-side of (14) signifies that high stresses promote cell death. Equation (14) represents the relation between tumor growth and stress and for $\eta_1 = \eta_2 = 0$ we recover the growth equation of Ngwa and Agyingi (2012)[28] as a particular case.

Now, as a consequence of tumor incompressibility (assumption vi),

$$\frac{\partial \rho}{\partial t} + \boldsymbol{v} \cdot \nabla \rho = \dot{\rho} = 0,$$

and substituting in (14), we obtain

$$\nabla \cdot \boldsymbol{v} = \alpha c (1 - \eta_1 \sqrt{\boldsymbol{\sigma}:\boldsymbol{\sigma}}) - k(1 + \eta_2 \sqrt{\boldsymbol{\sigma}:\boldsymbol{\sigma}}). \tag{16}$$

2.5. *Nutrient concentration*

The nutrient concentration variation is determined by nutrient diffusion through the tumor boundary and its consumption by the tumor cells in the interior

$$nutrient\ variation = diffusion - consumption.$$

Following the steps in Ward and King (1997)[48], combining hypothesis v) with Fick's law of diffusion and the mass balance equation, yields

$$\frac{\partial c}{\partial t} + \nabla \cdot (c\boldsymbol{v}) = \underbrace{D_c \nabla^2 c}_{diffusion} - \underbrace{\frac{A_c}{\rho_0} c\rho}_{consumption}, \tag{18}$$

where c represents the nutrient concentration; D_c and A_c/ρ_0 denote the constant diffusion coefficient and the nutrient consumption rate, respectively, while ρ_0 is the density at the initial time. Moreover, in the non-dimensionalization process it is shown that the left side of equation (18) has

a magnitude of αc_b, and because of the slow process of cell division, it is much smaller than the magnitude of the right side. Hence, similarly as was done in Ngwa and Agyingi (2012) [28], and in Ward and King (1997) [48] we have from Eq. (18)

$$\begin{aligned} D_c \nabla^2 c &= \frac{A_c}{\rho_0} c\rho \\ &= A_c c \quad \textit{because of tumor incompressibility.} \end{aligned} \tag{19}$$

Equation (19) represents the nutrient concentration variation.

2.6. *Non-dimensional form of the equations*

It is convenient to introduce dimensionless variables. For this purpose, the following scaling constants are defined

$$L \equiv \sqrt{\frac{D_c}{(A_c/\rho_0)\rho}}, \;\; \tau \equiv \frac{1}{\alpha c_b}, \;\; c_b, \;\; \epsilon \equiv \frac{k}{\alpha c_b},$$

which represent the length scale, time scale, constant nutrient concentration at the boundary, and ratio between death and cell proliferation rates, respectively. Using asterisks to identify dimensionless variables,

$$r^* = \frac{r}{L}, \;\; \sigma_{ij}^* = \frac{\sigma_{ij}}{E}, \;\; p^* = \frac{p}{E}, \;\; v_r^* = \frac{v_r}{\alpha c_b L}, \;\; t^* = \frac{t}{\tau}, \;\; c^* = \frac{c}{c_b}, \;\; \zeta_1 \equiv \eta_1 E, \;\; \zeta_2 \equiv \eta_2 E, \tag{21}$$

where the physical quantities of mass $[M]$, length $[L]$ and time $[T]$ in each one of the variables are:

$$\rho = \frac{[M]}{[L]^3}, \;\; D_c = \frac{[L]^2}{[T]}, \;\; A_c/\rho_0 = \frac{[L]^3}{[M][T]}, \;\; k = \frac{1}{[T]}, \;\; \alpha = \frac{1}{[T]}, \;\; E = \sigma_{ij} = \lambda = p = \frac{[M]}{[L][T]^2}.$$

We non-dimensionalize equations (3), (5), (10), (11), (19) and (16) by means of the newly introduced variables (cf. equation (21)). Therefore, taking into account radial symmetry and removing asterisks for the sake of clarity, equation (3) remains without changes

$$\frac{dR}{dt} = v_r(R, t).$$

Equation (19) becomes

$$\frac{1}{r^2}\frac{\partial}{\partial r}\left(r^2 \frac{\partial c}{\partial r}\right) = c, \tag{24}$$

subject to the boundary conditions $c = 1$ at the tumor boundary and $\frac{\partial c}{\partial r} = 0$ at $r = 0$, due to the radial symmetry.

From (16), since $\boldsymbol{v} = (v_r, 0, 0)$, we have

$$\frac{1}{r^2}\frac{\partial}{\partial r}(r^2 v_r) = c\left(1 - \zeta_1\sqrt{\boldsymbol{\sigma}:\boldsymbol{\sigma}}\right) - \epsilon\left(1 + \zeta_2\sqrt{\boldsymbol{\sigma}:\boldsymbol{\sigma}}\right), \tag{25}$$

subject to $v_r = 0$ at $r = 0$.

From (5) the same equation holds. From (10) we obtain,

$$\left(\frac{\partial}{\partial t} + v_r\frac{\partial}{\partial r}\right) g = c\left(1 - \zeta_1\sqrt{\boldsymbol{\sigma}:\boldsymbol{\sigma}}\right) - \epsilon\left(1 + \zeta_2\sqrt{\boldsymbol{\sigma}:\boldsymbol{\sigma}}\right). \tag{26}$$

The only relevant component of (11) reads

$$\frac{\partial v_r}{\partial r} = \frac{1}{r^2}\frac{\partial}{\partial r}(r^2 v_r)\gamma_r + g\frac{D\gamma_r}{Dt} + \frac{1}{2}\left(\frac{\partial}{\partial t} + v_r\frac{\partial}{\partial r}\right)(2\sigma_r - \sigma_\theta - \sigma_\phi), \tag{27}$$

since the second and third equation in (11) are redundant with the first one when radial symmetry is considered.

2.7. *Further simplifications*

The substitution $c = q/r$ is made in (24), leading to an ordinary differential equation which is solved for q. Then, the solution of (24) is

$$c(r,t) = \frac{R\sinh r}{r\sinh R}. \tag{28}$$

Then, substituting (28) into (25),

$$\begin{aligned}\frac{\partial v_r}{\partial r}(r,t) = {} & \frac{R\sinh(r)}{r\sinh(R)}\left(1 - \zeta_1\sqrt{\sigma_r^2(r,t) + 2\sigma_\theta^2(r,t)}\right) - \epsilon\left(1 + \zeta_2\sqrt{\sigma_r^2(r,t) + 2\sigma_\theta^2(r,t)}\right) \\ & - 2\frac{v_r(r,t)}{r}.\end{aligned} \tag{29}$$

In the same way, the subtitution of (28) in (26) leads to

$$\left(\frac{\partial}{\partial t} + v_r\frac{\partial}{\partial r}\right)g = \frac{R\sinh(r)}{r\sinh(R)}\left(1 - \zeta_1\sqrt{\sigma_r^2(r,t) + 2\sigma_\theta^2(r,t)}\right) - \epsilon\left(1 + \zeta_2\sqrt{\sigma_r^2(r,t) + 2\sigma_\theta^2(r,t)}\right). \tag{30}$$

Moreover, using representation (8) in equations (5) and (27), they are rewritten as

$$\frac{\partial \sigma_r}{\partial r} + \frac{2\beta}{r} = 0, \tag{31}$$

$$g\frac{D\gamma_r}{Dt} + \left(\frac{\partial}{\partial t} + v_r\frac{\partial}{\partial r}\right)\beta = 2\left(\gamma_\theta\frac{\partial v_r}{\partial r} - \gamma_r\frac{v_r}{r}\right). \tag{32}$$

In particular, substituting (9) in (32), we have

$$\left(\frac{\partial}{\partial t} + v_r\frac{\partial}{\partial r}\right)\beta = \varpi, \tag{33}$$

where

$$\begin{aligned}\varpi = {} & \frac{2}{1 + 2ag\frac{e^{a\beta}}{(e^{a\beta}+2)^2}}\left(\gamma_\theta\frac{\partial v_r}{\partial r} - \gamma_r\frac{v_r}{r}\right) = \frac{2}{1 + 2ag\frac{e^{a\beta}}{(e^{a\beta}+2)^2}}\left(\gamma_\theta\frac{\partial v_r}{\partial r} + (2\gamma_\theta - 1)\frac{v_r}{r}\right) \\ = {} & \frac{1}{1 + 2ag\frac{e^{a\beta}}{(e^{a\beta}+2)^2}}\left[-\frac{e^{a\beta}}{e^{a\beta}+2}\left(\frac{R\sinh(r)}{r\sinh(R)}\left[1 - \zeta_1\sqrt{\sigma_r^2(r,t) + 2(\sigma_r(r,t) - \beta(r,t))^2}\right]\right.\right. \\ & - \left.\left.\epsilon\left[1 + \zeta_2\sqrt{\sigma_r^2(r,t) + 2(\sigma_r(r,t) - \beta(r,t))^2}\right]\right) + \frac{\partial v_r}{\partial r}\right].\end{aligned}$$

In order to solve equations (31) and (33), conditions for β and σ_r are needed. As in these equations the only derivative of σ_r is the first spatial derivative in (31), we need a condition for σ_r over a curve non-constant in time. But, (33) is a hyperbolic equation of first order for β, thus, even when the condition $\beta(r,0) \equiv 0$ is sufficient theoretically, for the numerical method explained later conditions for β at the boundaries of its domain are required.

1. The equations of the characteristic curves of (33) can be written as

$$\frac{dt}{1} = \frac{dr}{v_r} = \frac{d\beta}{\varpi},$$

i.e.,

$$\frac{d\beta}{dt} = \varpi \quad \text{and} \quad \frac{dr}{dt} = v_r.$$

Then, $r = 0$ is a characteristic of equation (33) and we obtain

$$\frac{d\beta}{dt}(0,t) = \lim_{r\to 0} \varpi(r,t) = 0.$$

Therefore, the first boundary condition for β is

$$\beta(0,t) = 0. \tag{35}$$

2. Condition for β at $r = R$:

In the same way as above, $r = R$ correspond to the other characteristic of (33). So, by taking

$$\frac{d\beta}{dt} = \varpi, \text{ for } r = R, \tag{36}$$

a characteristic curve is obtained and hence, the second boundary condition.

3. Condition for σ_r:

This condition may be determined if the constitutive equation (12) of the external medium is used assuming stress continuity at the tumor boundary. Because of the spherical tumor symmetry, the displacement vector is $\mathbf{u} = (u_r, 0, 0)$. Also, by the incompressibility of the external medium (hypothesis viii),

$$tr(\mathbf{e}) = \frac{1}{r^2}\frac{\partial}{\partial r}(r^2 u_r) = 0,$$

leading to

$$u_r = \frac{A}{r^2},$$

where A only dependes on t. Substituting this result in (12),

$$\begin{cases} \sigma_r^e = -p + \frac{2}{3}e_r^e = -p - \frac{4A}{3r^3} \\ \\ \sigma_\theta^e = \sigma_\phi^e = -p + \frac{2}{3}e_\theta^e = -p - \frac{2A}{3r^3} \end{cases}$$

and from the equilibrium condition (4), we have $p = constant$ and as for $p_\infty = 0$, this implies that $p = 0$.

Now, as the real initial radius of the tumor is zero, because at the very beginning of cancer appearance the tumor does not have any radius, then $u_r|_{r=R(t)} = R(t)$, implying that $A = R^3(t)$, and therefore

$$\sigma_r|_{r=R(t)} = -\frac{4}{3}. \tag{40}$$

2.8. *Mathematical model*

The mathematical model is given by equations (3), (29), (31) and (33), i.e., the final system of equations to be solved is

$$\frac{dR}{dt}(t) = v_r(R,t), \text{ for } t \in \mathbb{R}_+, \tag{41}$$

$$\frac{\partial v_r}{\partial r}(r,t) = \frac{R\sinh(r)}{r\sinh(R)}[1-\zeta_1\sqrt{\sigma_r^2(r,t)+2(\sigma_r(r,t)-\beta(r,t))^2}] - \epsilon[1+\zeta_2\sqrt{\sigma_r^2(r,t)+2(\sigma_r(r,t)-\beta(r,t))^2}] - 2\frac{v_r(r,t)}{r}, \text{ for } t \in \mathbb{R}_+^* \text{ and } r \in (0,R], \tag{42}$$

$$\frac{\partial \sigma_r}{\partial r}(r,t) = -\frac{2\beta}{r}, \text{ for } t \in \mathbb{R}_+^* \text{ and } r \in (0,R], \tag{43}$$

$$\frac{\partial g}{\partial t}(r,t) = -v_r(r,t)\frac{\partial g}{\partial r}(r,t) + \frac{R\sinh(r)}{r\sinh(R)}\left(1-\zeta_1\sqrt{\sigma_r^2(r,t)+2(\sigma_r(r,t)-\beta(r,t))^2}\right) - \epsilon\left(1+\zeta_2\sqrt{\sigma_r^2(r,t)+2(\sigma_r(r,t)-\beta(r,t))^2}\right), \text{ for } t \in \mathbb{R}_+ \text{ and } r \in [0,R], \tag{44}$$

$$\frac{\partial \beta}{\partial t}(r,t) = -v_r(r,t)\frac{\partial \beta}{\partial r}(r,t) + \varpi(r,t), \text{ for } t \in \mathbb{R}_+^* \text{ and } r \in [0,R], \tag{45}$$

with

$$\varpi(r,t) = \frac{1}{1+2ag(r,t)\frac{e^{a\beta(r,t)}}{(e^{a\beta(r,t)}+2)^2}}\left[-\frac{e^{a\beta(r,t)}}{e^{a\beta(r,t)}+2}\left(\frac{R\sinh(r)}{r\sinh(R)}\left[1-\zeta_1\sqrt{\sigma_r^2(r,t)+2(\sigma_r(r,t)-\beta(r,t))^2}\right] - \epsilon\left[1+\zeta_2\sqrt{\sigma_r^2(r,t)+2(\sigma_r(r,t)-\beta(r,t))^2}\right]\right) + \frac{\partial v_r}{\partial r}\right], \tag{46}$$

subject to initial and boundary conditions

$$R(0) = R_0, \tag{47}$$

$$v_r(0,t) = 0, \tag{48}$$

$$\sigma_r(R(t),t) = -\frac{4}{3}, \tag{49}$$

$$g(r,0) = 1, \tag{50}$$

$$\beta(r,0) = 0. \tag{51}$$

The initial condition for g is just an arbitrary value because of the lack of references. For the numerical solution of g similar boundary conditions to those for β can be derived.

3. Results and discussion

The results of the mathematical model are presented in this section for two types of tumor growth: a) anisotropic growth without growth-stress dependence and b) anisotropic growth with growth-stress dependence. In particular, the influence of the parameters γ_θ and ζ_1, accounting for anisotropy and growth-stress dependence, respectively, on tumor growth behavior is studied. The figures shown in this section contain dimensionless variables, so the results must be interpreted only qualitatively. In particular, the following parameters are fixed: $R_0 = 1$ and $\epsilon = 0.1$ (ratio of proliferation and death rate). In Montel et al. (2012) [27], it is shown that apoptosis induction by compressive forces is much less than the effects of cell division inhibition. Hence, the parameter ζ_2 in equation (14), accounting for the dependence of apoptosis on stress, is considered a few magnitude orders less than ζ_1 (ζ_1 represents the dependence of cell proliferation on stress). In particular,

we assume that $\zeta_2 = 10^{-2}\zeta_1$. The parameter a of the anisotropic growth term γ_θ, representing the sensitivity of growth directions on stresses, is not fixed and will vary according to the simulations.

Parameter	Value
R_0	1
ϵ	0.1
a	is specified in each simulation
ζ_1	is specified in each simulation
ζ_2	$\zeta_1/100$

Table 3: Parameters used for the numerical simulations.

3.1. *Numerical methods*

In order to solve the system (41)-(45), we use a combination of numerical methods. The modified Euler method or Heun's method [14] is used for (41). For equations (42) and (43) the trapezoids method [15] is used after rewriting (42) and (43) in integral form. A modified Lax-Wendroff finite difference scheme [21;28] is employed to calculate β in equation (45). As equation (44) for g has the same structure of (45), the same method is employed.

In its original form, the Lax-Wendroff method [23] is applied to a fixed region in the space. But, by including a modification in the second order approximation of the function, this is extended to a variable integration region. The approximated solution is calculated at the points from the lattice in the plane $r \times t$ defined by

$$r_i = ih,\ i = 0, 1, 2, ..., i_{max},$$
$$t_j = jk,\ j = 0, 1, 2, ..., j_{max},$$

where h and k are the spatial and time steps size, respectively. The number of spatial points $i_{max} + 1$ is fixed. However, the step size h depends on time and it is calculated as $h = R(t)/i_{max}$. The Lax-Wendroff method consists in approximating β at the instant t_{j+1} by its Taylor series expansion with respect to time evaluated at the instant t_j

$$\beta(r_i, t_{j+1}) = \beta(r_i, t_j) + \frac{\partial\beta}{\partial t}(r_i, t_j)k + \frac{\partial^2\beta}{\partial t^2}(r_i, t_j)\frac{k^2}{2} + O(k^3), \tag{52}$$

and then, using equation (45), the temporal derivatives are substituted by their spatial derivatives

$$\frac{\partial\beta}{\partial t} = -v_r\frac{\partial\beta}{\partial r} + \varpi, \tag{53}$$
$$\frac{\partial^2\beta}{\partial t^2} = -\frac{\partial v_r}{\partial t}\frac{\partial\beta}{\partial r} + v_r\frac{\partial v_r}{\partial r}\frac{\partial\beta}{\partial r} + v_r^2\frac{\partial^2\beta}{\partial r^2} - v_r\frac{\partial\varpi}{\partial r} + \frac{\partial\varpi}{\partial t}. \tag{54}$$

But, points r_i are not the same at each time instant because h depends on time. Then, the approximation by the Taylor series of β at the point $(r_i^{(j+1)}, t_{j+1})$ is given by

$$\begin{aligned}\beta(r_i^{(j+1)}, t_{j+1}) &= \beta(r_i^{(j)} + (R(t_{j+1}) - R(t_j))i/i_{max}, t_j + k)\\ &\approx \beta(r_i^{(j)}, t_j) + \frac{\partial\beta}{\partial r}(R(t_{j+1}) - R(t_j))\frac{i}{i_{max}} + \frac{\partial\beta}{\partial t}(r_i^{(j)}, t_j)k\\ &+ \frac{\partial^2\beta}{\partial r^2}(R(t_{j+1}) - R(t_j))^2\frac{i^2}{2i_{max}^2} + \frac{\partial^2\beta}{\partial r\partial t}(R(t_{j+1}) - R(t_j))\frac{i}{i_{max}}k\end{aligned}$$

$$+ \frac{\partial^2 \beta}{\partial t^2}(r_i^{(j)}, t_j)\frac{k^2}{2}. \tag{55}$$

In the same way as in (52), the time derivatives in (55) must be substituted by formulas (53) and (54), and the spatial derivatives of β are approximated by

$$\frac{\partial \beta}{\partial r}(r_i^{(j)}, t_j) = \frac{\beta(r_{i+1}^{(j)}, t_j) - \beta(r_{i-1}^{(j)}, t_j)}{2h},$$
$$\frac{\partial^2 \beta}{\partial r^2}(r_i^{(j)}, t_j) = \frac{\beta(r_{i+1}^{(j)}, t_j) - 2\beta(r_i^{(j)}, t_j) + \beta(r_{i-1}^{(j)}, t_j)}{h^2}.$$

The derivatives of v_r and ϖ with respect to r and t can be approximated using a finite differences scheme. It should be noted that approximation (55) is only true for the interior points of the region. To calculate the solution at the boundary, equations (35) and (36) must be used.

Then, for each time instant t_j, the order of the calculations is as follows. First,

$$\sigma(r_i^j, t_j), \quad i = \overline{0, i_{max}},$$

is computed, and it is used to determine

$$v_r(r_i^j, t_j), \quad i = \overline{0, i_{max}},$$

and after compute v_r, R is evaluated at t_{j+1}, and

$$\beta(r_i^{j+1}, t_{j+1}) \quad \text{and} \quad g(r_i^{j+1}, t_{j+1}) \quad i = \overline{0, i_{max}},$$

are estimated at the same step.

An important feature of numerical methods is their stability, since it describes the propagation of the errors of the results. As was specified above, the system (41)-(45) is composed of five coupled and nonlinear differential equations. Thus, a rigorous study of the stability of the discrete solutions is not easy. Here, we analyze each equation by separately assuming that we have the real values of the other four functions. That is to say, if we want to explore the stability of the numerical method used for equation (41) of R, the exact values of $v_r,\ \sigma_r,\ g,\ \beta$ are assumed known, and so on with the other equations.

Following these considerations, the stability of the numerical method for the ordinary differential equation (41), given that the non homogeneous term is bounded, corresponds to a simpler case of the stability test model from Farago (2013) [14]. Now, as equations (42) and (43) are computed as integrals in well delimited intervals at each instant of time, there is no problem with their stability. On the other hand, since in the equations for β and g appear terms of the form k/h_j with $h_j = R(t_j)/i_{max}$, this suggests that an unsuitable selection of k and h_j could result in a bad behavior of the numerical method.

By substituting equations (53) and (54) and those of the partial derivatives of β in (55), we obtain

$$\beta(r_i^{(j+1)}, t_{j+1}) = \beta(r_i^j, t_j)\left[1 - \frac{k^2}{h_j^2}\left((R(t_{j+1}) - R(t_j))\frac{i}{i_{max}} - v(r_i^j, t_j)\right)^2\right]$$
$$+ \beta(r_{i-1}^j, t_j)\left[\frac{k^2}{2h_j^2}\left((R(t_{j+1}) - R(t_j))\frac{i}{i_{max}} - v(r_i^j, t_j)\right)^2\right.$$

$$
\begin{aligned}
&- \frac{k}{2h_j}\left((R(t_{j+1})-R(t_j))\frac{i}{i_{max}} - v(r_i^j,t_j)\right)\\
&- \frac{k^2}{2h_j}\left(v_r(r_i^j,t_j)(R(t_{j+1})-R(t_j))\frac{i}{i_{max}} - \frac{v(r_i^j,t_j)v_r(r_i^j,t_j)-v_t(r_i^j,t_j)}{2}\right)\Bigg]\\
&+ \beta(r_{i+1}^j,t_j)\left[\frac{k^2}{2h_j^2}\left((R(t_{j+1})-R(t_j))\frac{i}{i_{max}} - v(r_i^j,t_j)\right)^2\right.\\
&+ \frac{k}{2h_j}\left((R(t_{j+1})-R(t_j))\frac{i}{i_{max}} - v(r_i^j,t_j)\right)\\
&+ \left.\frac{k^2}{2h_j}\left(v_r(r_i^j,t_j)(R(t_{j+1})-R(t_j))\frac{i}{i_{max}} - \frac{v(r_i^j,t_j)v_r(r_i^j,t_j)-v_t(r_i^j,t_j)}{2}\right)\right],\\
&+ k\left[\varpi(r_i^j,t_j) + k\left(\frac{\partial\varpi}{\partial r}(r_i^j,t_j)(R(t_{j+1})-R(t_j))\frac{i}{i_{max}}\right.\right.\\
&+ \left.\left.\frac{\frac{\partial\varpi}{\partial t}(r_i^j,t_j) - v(r_i^j,t_j)\frac{\partial\varpi}{\partial r}(r_i^j,t_j)}{2}\right)\right], \qquad (56)
\end{aligned}
$$

for $1 \leq i \leq i_{max}-1$. Since the last term multiplied by k correponds to the non-homogeneous part of the equation and it is bounded, it can be removed from the stability analisys [47]. Using the change of variables

$$\xi = \frac{k}{2h_j}\left((R(t_{j+1})-R(t_j))\frac{i}{i_{max}} - v(r_i^j,t_j)\right),$$

equation (56) leads to

$$\beta(r_i^{(j+1)},t_{j+1}) = \beta(r_i^j,t_j)\left(1-4\xi^2\right)+\beta(r_{i-1}^j,t_j)\left(2\xi^2-\xi-kO(\xi)\right)+\beta(r_{i+1}^j,t_j)\left(2\xi^2+\xi+kO(\xi)\right), \qquad (57)$$

for $i = \overline{1, i_{max}-1}$. Hence, k can be picked small enough that the signs of the multipliers of $\beta(r_{i-1}^j,t_j)$ and $\beta(r_{i+1}^j,t_j)$ depend only on $2\xi^2-\xi$ and $2\xi^2+\xi$, respectively. This is possible since the functions in $O(\xi)$ are bounded. Bearing this in mind, if $\xi \in (-1/2,0)$ then

$$1-4\xi^2 > 0,\ 2\xi^2-\xi < 0,\ 2\xi^2+\xi > 0,$$

and from equation (57)

$$
\begin{aligned}
\max_{1\leq i\leq i_{max}-1}|\beta(r_i^{j+1},t_{j+1})| &\leq \max_{1\leq i\leq i_{max}-1}|\beta(r_i^j,t_j)|(1-4\xi^2+2\xi+2kO(\xi))+O(k)\\
&\leq \max_{1\leq i\leq i_{max}-1}|\beta(r_i^j,t_j)|, \text{ since } \xi\in(-1/2,0).
\end{aligned}
$$

On the other hand, if $\xi \in (0,1/2)$ then

$$1-4\xi^2 > 0,\ 2\xi^2-\xi > 0,\ 2\xi^2+\xi < 0,$$

and from equation (57) we obtain

$$
\begin{aligned}
\max_{1\leq i\leq i_{max}-1}|\beta(r_i^{j+1},t_{j+1})| &\leq \max_{1\leq i\leq i_{max}-1}|\beta(r_i^j,t_j)|(1-4\xi^2-2\xi-2kO(\xi))\\
&\leq \max_{1\leq i\leq i_{max}-1}|\beta(r_i^j,t_j)|, \text{ since } \xi\in(0,1/2).
\end{aligned}
$$

The case where $\xi = 0$ is trivial. So, following the criteria from Thomas (1995) [47], the conditions $\xi \in (-1/2,1/2)$ and k small enough such that $kO(\xi)$ does not have almost influence compared with ξ are sufficient to guarantee the stability of the modified Lax-Wendroff scheme. For the boundary

conditions of β, one of them is trivial and the other corresponds to the same above observation for equation (41) of R.

Actually, for the simulations performed in the following section, a time step $k = 0.03$ with a spatial partition of $i_{max} = 350$ suffices. Moreover, in order to find v_r a smaller spatial step size at a vicinity of $r = 0$ is considered in order to increase the accuracy of the term v_r/r in this region.

3.2. *Isotropic and anisotropic growth without stress-dependence*

Figure 1 shows the evolution of the tumor radius, with parameter values $a = 0$ and $\zeta_1 = 0$, describing isotropic growth without growth-stress dependence. In Fig. 1 it is observed that the velocity of

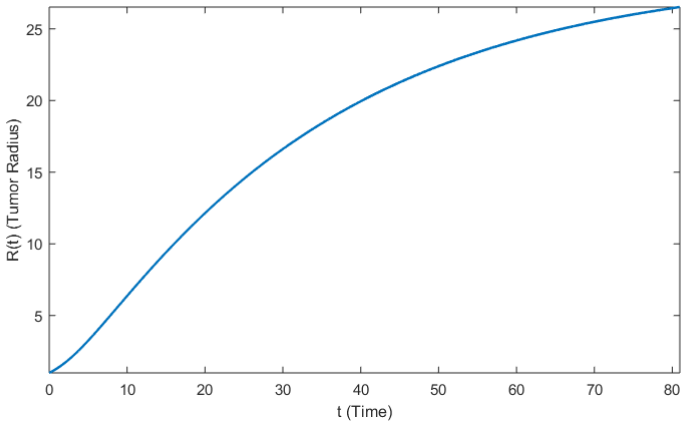

Fig. 1: Tumor radius evolution in the time interval $[0, 81]$ considering isotropic growth without growth-stress dependence.

the tumor radius is increasing at the begining and it presents an inflection point at $t \approx 10$, where the velocity diminishes, adopting a sigmoidal growth shape. This phenomenon could be explained by the struggle of the tumor displacing the elastic and isotropic external medium in order to grow, limiting the cell's division capability and promoting apoptosis while it continues its expansion until growth equilibrium is reached. In particular, Fig. 1 reproduces the growth described in Ngwa and Agyingi (2012)[28] for the same set of parameter values. Since we are not considering dependence of growth on stress, the radius distribution for different values of the parameter a, which is in turn related to γ_θ, is unchanged. Therefore, anisotropy does not influences growth but it does affect the stress distribution. In Fig. 2 the radial and transversal stresses at five fixed time instants ($t = 16, 32, 48, 65, 81$) are shown, for the values of the parameter $a = 0$ and $a = 1$. The former corresponds to isotropic growth, and the later accounts for anisotropic growth. The fact that almost all stresses are positive (tensile) near the origin could be the result of the cells dying in the interior of the tumor. Due to this empty space left by the dying cells a force is generated dragging the nearest cells to the center and therefore, stretching them. The negative stress (compressive) at the boundary could be explained as a result of the elastic nature of the external medium pushing the tumor surface in opposite direction to the expansive forces of the proliferating cells, and also, product of the proliferating cells pushing itselves against each other.

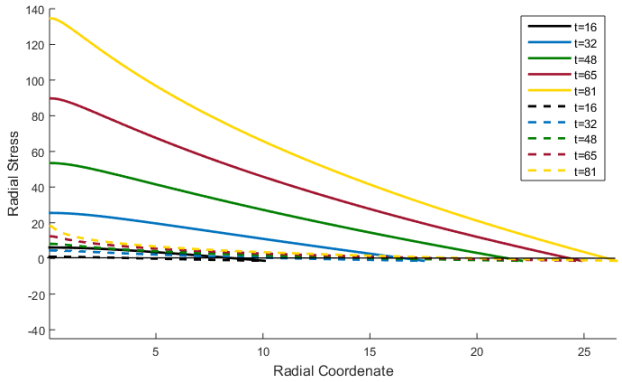

(a) Radial stress for $a = 0$ (solid) and $a = 1$ (dashed).

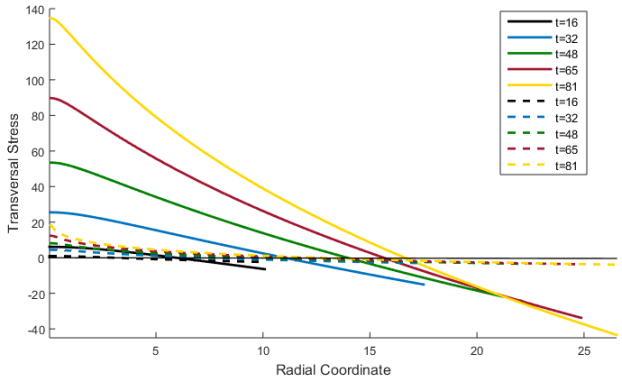

(b) Transversal stress for $a = 0$ (solid) and $a = 1$ (dashed).

Fig. 2: Radial and transversal stress at five fixed time instants ($t = 16, 32, 48, 65, 80$).

Moreover, Fig. 2 shows that radial and transversal stressess are much less tensile in the interior of the tumor for the parameter value $a = 1$ of the anisotropy term (dashed curves), and are less compressive at the boundary than those from isotropic growth (solid curves). This behavior implies that the parameter a, and so the anisotropic term, has a direct influence on the stress distribution. In particular, the results in Fig. 2 for the isotropic formulation coincide with those reported in Ngwa and Agyingi (2012) [28] (Fig. 1) and Jones et al. (2000) [21] (Fig. 6).

An interesting detail in Fig. 2 is that, at the center of the tumor, radial and transversal stresses have exactly the same values. From a mathematical point of view, this is because by equation (43) in order to ensure the existence of $\partial\sigma_r/\partial r$ in the solution domain, the function $\beta = \sigma_r - \sigma_\theta$ must be zero at $r = 0$. From the experimental measurements in Stylianopoulos et al. 2012 [42] radial and transversal stresses at the tumor center are observed to be extremely close between them. In the present model, the difference between radial and transversal stresses increases with the distance from the center of the tumor and also with time, for example, in Fig. 2 (a) and (b) solid yellow curves start to differentiate prior to the solid blue curves. But in general they have a similar behav-

ior, which is probably associated to the local linearity of the constitutive law. In the works dealing with a locally linear constitutive law analogous profiles of the stresses are reported [6;21;28]. On the other hand in those where nonlinear constitutive laws are considered, the radial and transversal stresses are significantly different [3;35;43].

3.3. *Isotropic and anisotropic stress-dependent growth*

Until now, results were limited to the condition $\zeta_1 = \zeta_2 = 0$, i.e., growth without dependence on stress. Figure 3 shows the tumor radius in the time interval $[0, 81]$ as a function of (a) the parameter a with $\zeta_1 = 0.002$ fixed, and (b) the growth stress-dependence parameter ζ_1 for $a = 1$.

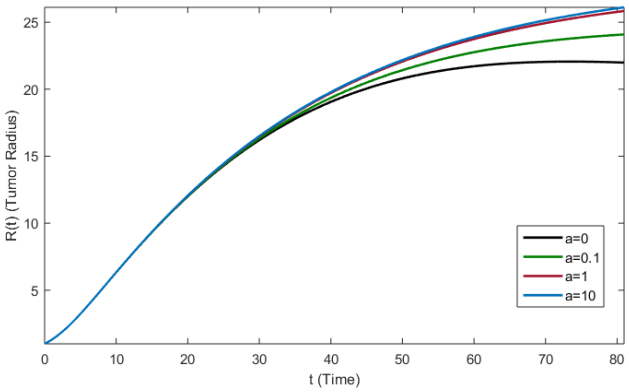

(a) Influence of anisotropy parameter on radius.

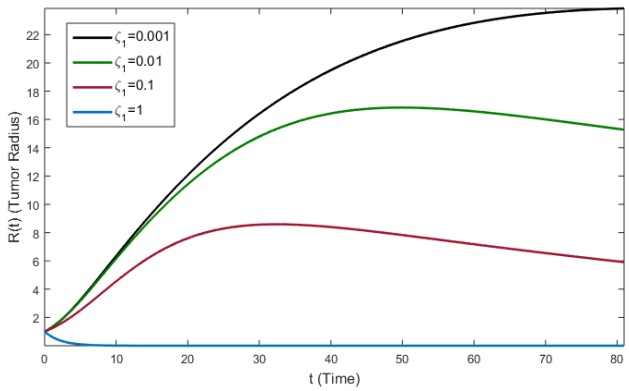

(b) Influence of growth-stress dependence parameter on radius.

Fig. 3: Tumor radius evolution for four different values of the parameters a and ζ_1 within the time interval $[0, 81]$.

In Fig. 3 (a) the tumor radius increases with the increase in the anisotropy parameter a, and the radius profile which corresponds to $\gamma_\theta = 0$ is rapidly approached according to relatioship (9). Then, the present study shows the importance of the anisotropy parameter γ_θ (when growth is

stress dependent) in the tumor evolution. On the other hand, according to Fig. 3 (b), the parameter ζ_1 seems to play a major role in determining the magnitude of the tumor radius. Also, it seems that there exists a value such that when ζ_1 is greater than this number, there is no growth at all (blue curve). This is due to the fact that an increase in ζ_1 causes an increase in the role played by the stress in limiting the cell proliferation (14). In fact, Fig. 3 (b) shows a regression of the tumor. This kind of behavior has been reported in Challis and Stam (1990) [11], Ricci and Cerchiari (2010) [37], and Roose et al. (2003) [38].

Now, in order to determine the influence of the parameters a and ζ_1 in the tumor growth, simulations were made in 320 equally spaced points in the rectangle $[0, 10] \times [0, 0.5]$ (see Fig. 4).

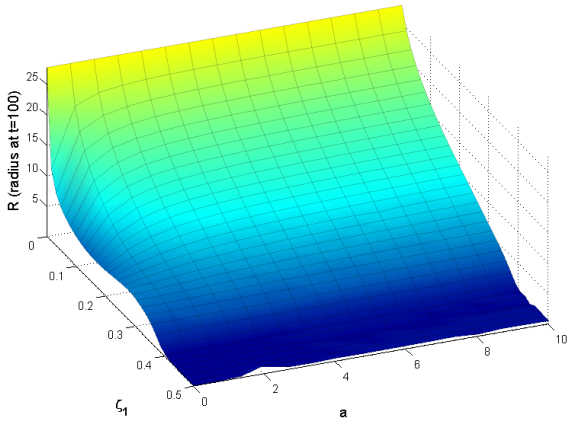

(a) Distribution of the tumor radius reached at the instant $t = 100$.

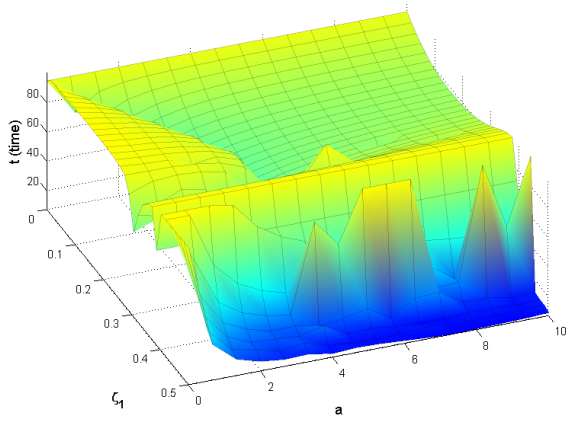

(b) Distribution of the time instants at which the tumor radius does not change onwards.

Fig. 4: Distributions based on the parameters a and ζ_1 of anisotropy and growth-stress dependence, respectively, in the region $\gamma_\theta, \zeta_1 \in [0, 10] \times [0, 0.5]$, for the time interval $t \in [0, 100]$. Warm colors means higher values in the z axis and cold colors means lower values.

In particular, in Fig. 4 (a), the tumor radius dependence on the parameter a is noted as was expected according to Fig. 3. The influence of a is more visible for values of ζ_1 near to zero, that is the radius reaches higher values for small values of ζ_1. On the other hand, although Fig. 4 (b) seems chaotic, it can be distinguished that for values of ζ_1 greater than 0.35, the time instant at which the tumor radius stabilizes is smaller compared with when ζ_1 approaches to zero, where the surface color turns yellow, because the time instant at which the tumor radius stabilizes increases.

In Fig. 3 (a) for a fixed value of ζ_1 it is displayed that the tumor grows more when anisotropic growth is considered. Fig. 5 shows the tumor growth for the same set of parameter values as in Fig. 3 (b), except for a, which is set to 1, corresponding to the anisotropic case. It is observed that the consideration of anisotropic growth, leads to larger tumor radius for different values of ζ_1. An explanation of this phenomenon could be that this type of anisotropic growth generates less stress, allowing a higher rate of cell proliferation and a lower rate of cell death. In fact, Fig. 6 (a) and (b) presents the radial and transversal stresses for the radius evolution (solid and dotted blue lines) exhibited in Fig. 5 for five different times. In Fig. 6 (b) the dashed lines, which describe

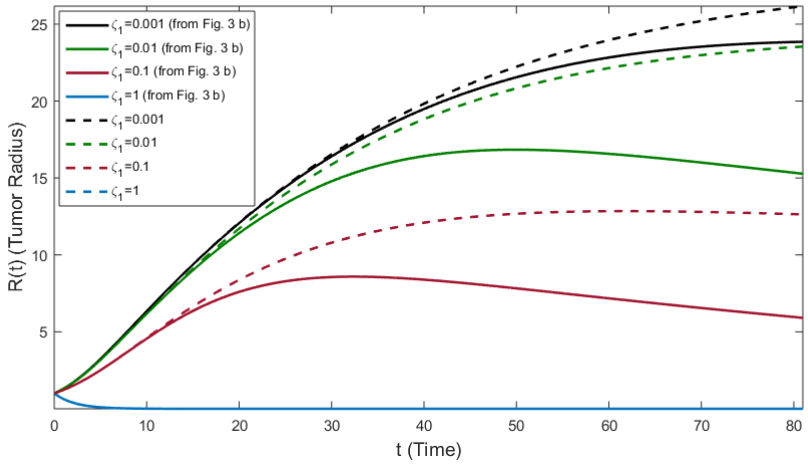

Fig. 5: Radius evolution for four different values of the parameter ζ_1 of growth-stress dependence at the time interval $[0, 81]$. The solid lines describe the radius evolution when equation (9) is adopted. The dot lines are the same from Fig. 3 (b).

transversal stress, are much less tensile in the tumor interior and less compressive near the tumor boundary respect to the solid lines. A similar tendency and behavior is noticed in Fig. 6 (a), where the radial stress generated with $a = 1$ is smaller than the one generated assuming isotropic growth, i.e. for $a = 0$. These results make clear the stress relaxation consequences studied by Araujo and McElwain (2005b) [8]. Moreover, the outcomes in Fig. 3 are in accordance with the explanation that low stress levels imply higher tumor radius.

In all the simulations, the radial and tranversal stresses are positive in the tumor interior and decrease as the distance from the center of the tumor increases until they reach negative values

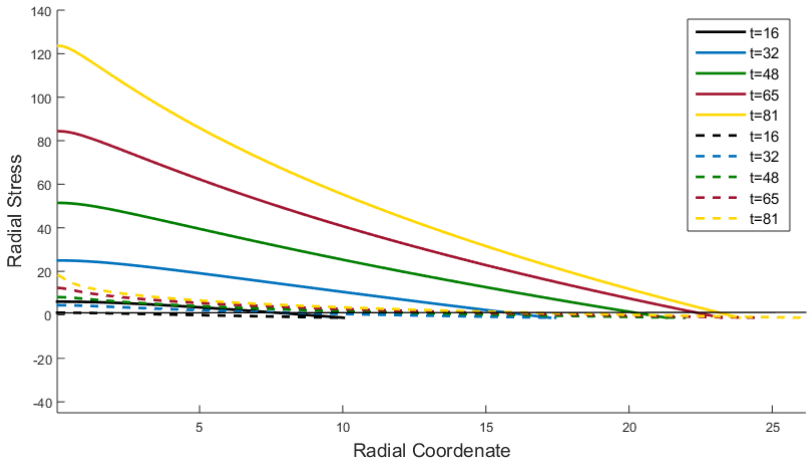

(a) Radial stress for $a = 0$ (solid) and $a = 1$ (dashed).

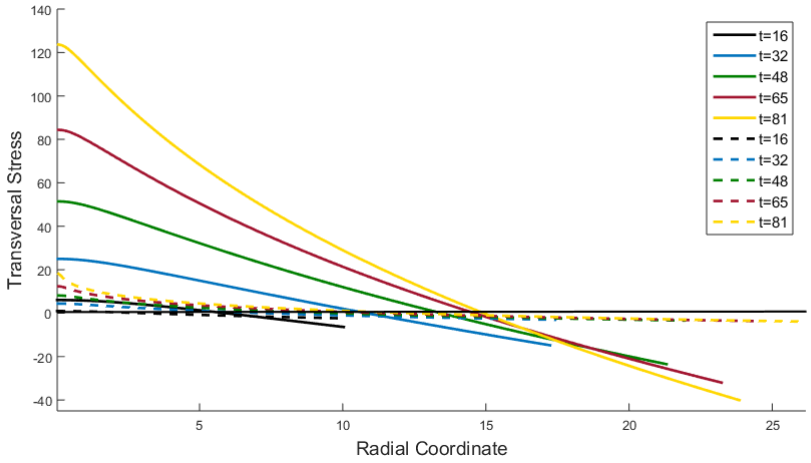

(b) Transversal stress for $a = 0$ (solid) and $a = 1$ (dashed).

Fig. 6: Radial and transversal stress at five time instants ($t = 16, 32, 48, 65, 80$).

(see Fig. 2 and Fig. 6). In principle, it may seem contradictory with the previous works from Stylianopoulos et al. 2012 [42] and Stylianopoulos et al. 2013 [43] where experimental measurements in *ex-vivo* conditions were done, and their results point out the existence of negative stresses in the tumor interior and positive stresses at the tumor outer layer. But there are two main differences between those studies and this one. The first one consists that the tumor modeled by Stylianopoulos et al. 2012 [42], Stylianopoulos et al. 2013 [43] and the experimental measurements are made in vascularized tumors whereas the present model deals with avascular tumor. The importance of this feature can be observed in the work of Araujo and McElwain 2004 [6], where they model an avascular tumor and obtain similar behavior of the stresses to the ones of this study. In other work, Araujo and McElwain 2005 [7], considered the tumor vascularization only, and negative stress distribution at the tumor interior were obtained. These evidences suggest that the experimental observations of a vascularized tumor cannot be extrapolated to an avascular tumor. The second

difference resides that in the mathematical model of Stylianopoulos et al. 2013 [43] the constitutive equation is nonlinear whereas in the current study, as it was explained in Subsection 2.2, locally the elastic response is linear with respect to the change in strain but globally is nonlinear because of the convective effects. In Ramírez-Torres et al. [35], an avascular tumor is modeled with a locally nonlinear constitutive law. In particular, negative radial stresses are obtained at the tumor center if an anisotropic growth law is taken into account. Therefore, the locally nonlinearity of the constitutive equation seems to be important too.

4. Conclusions

The presented model may be considered as a generalization of the work of Ngwa and Agyingi (2012) [28], which is extended to anisotropic growth and the dependence of growth on stress. Moreover, Ngwa and Agyingi (2012) [28] model can be recovered as a particular case of the proposed mathematical model in this work for specific values of the parameters a and ζ, assuming isotropic growth and without stress dependence. One of the results of this study is the description of the influence of the parameters on the final tumor radius via a parametric analysis, which highlights the region characterized by the highest sensitivity to changes in the parameters. On the other hand, when no growth-stress dependence was considered, significant stress distribution changes for different values of the anisotropy parameter a were reached. In particular, the numerical results agreed with those in Araujo and McElwain (2005b) [8]. Moreover, with growth-stress dependence, several magnitude and types of radius evolution behavior were achieved for parameter variations of growth stress-dependence ζ_1 and the anisotropy parameter a, respectively. Once having established the importance of anisotropic growth, the anisotropy parameter was considered as a stress function, allowing a stress relaxation effect described in Araujo and McElwain (2005b) [8], where it was shown that the effect of stress relaxation in growth leads to higher cell proliferation and lower cells death rates. Hence, it can be established that under this model considerations, the cell proliferation dependence on stress and the anisotropic growth nature are decisive mechanisms in the tumor evolution. Further developments include the consideration of (a) heterogeneities (Ramírez-Torres et al. (2017) [36]), (b) nonlinear rheology for the tumor (Ramírez-Torres et al. (2017) [35]), (c) vascularization (Penta et al. (2015) [31], (2017) [33]).

Acknowledgments

FV thanks to professors M. Ngwa and E. Agyingi for the help in the understanding of their paper. AR gratefully acknowledges the Program of Postdoctoral Scholarships of DGAPA from UNAM, Mexico. Since February AR is financially supported by INdAM. RR, RG and JB, thanks to the Project (7515) Métodos Físico-Matemáticos para el estudio de nuevos materiales y la propagación de ondas. Aplicaciones. JM and RP acknowledges support from the Ministery of Economy in Spain under the project reference DPI2014-58885-R. FJ thanks to Departamento de Matemáticas y Mecánica IIMAS-UNAM for their support and Ramiro Chávez Tovar and Ana Pérez Arteaga for computational assistance.

References

1. American Association for Cancer Research, 2015. *AACR Cancer Progress Report 2015*. Clinical Cancer Research 21, Supplement 1. SI-S128.

2. Ambrosi D, Mollica F, 2004. *The role of stress in the growth of a multicell spheroid.* Journal of Mathematical Biology, 48:477-99. doi:10.1007/s00285-003-0238-2
3. Ambrosi D, Preziosi L, Vitale G, 2012. *The interplay between stress and growth in solid tumors.* Mechanics Research Communications, 42:87-91. doi:10.1016/j.mechrescom.2012.01.002
4. Anderson A, 2005. *A hybrid mathematical model of solid tumor invasion: the importance of cell adhesion.* Mathematical Medicine and Biology, 22:163-186. doi:10.1093/imammb/dqi005
5. Andor N, Graham T, Jansen M, Xia L, Aktipis A, Petritsch C, Ji H, Maley C, 2016. *Pan-cancer analysis of clonal evolution reveals the costs and adaptive benefits of genomic instability.* Cancer Research, 76(14 Suppl), Abstract 2387. doi:10.1158/1538-7445.AM2016-2387
6. Araujo R, McElwain DLS, 2004. *A linear-elastic model of anisotropic tumour growth.* European Journal of Applied Mathematics, 15:365-384. doi:10.1017/S0956792504005406
7. Araujo R, McElwain DLS, 2005. *The role of mechanical hosttumour interactions in the collapse of tumour blood vessels and tumour growth dynamics.* Journal of Theoretical Biology, 238:817-827. doi:10.1016/j.jtbi.2005.06.033
8. Araujo R, McElwain DLS, 2005. *The nature of the stresses induced during tissue growth.* Applied Mathematics Letters, 18:1081-1088. doi:10.1016/j.aml.2004.09.019
9. Byrne H, Drasdo D, 2009. *Individual-based and continuum models of growing cell populations: a comparison.* Journal of Mathematical Biology, 58:657-87. doi:10.1007/s00285-008-0212-0
10. Carmenate T, Pacios A, Enamorado M, Moreno E, García K, Fuente D, León K, 2013. *Human IL-2 Mutein with Higher Antitumor Efficacy Than Wild Type IL-2.* Journal of Immunology, 190:6230-6238. doi:10.4049/jimmunol.1201895
11. Challis GB, Stam HJ, 1990. *The Spontaneous Regression of Cancer. A review of cases from 1900 to 1987.* Acta Oncologica, 29:545-50. doi:10.3109/02841869009090048
12. Cheng G, Tse J, Jain RK, Munn LL, 2009. *Micro-environmental mechanical stress controls tumor spheroid size and morphology by suppressing proliferation and inducing apoptosis in cancer cells.* PLoS One 4, e4632. doi:10.1371/journal.pone.0004632
13. Drasdo D, Hohme S, 2005. *A single-cell-based model of tumor growth in vitro: monolayers and spheroids.* Physical Biology, 12:133-47. doi:10.1088/1478-3975/2/3/001
14. Faraó I, 2013. *Numerical Methods for Ordinary Differential Equations.* url: http://www.cs.elte.hu/∽faragois/ODE_angol.pdf, last access 5 of June from 2017.
15. Faires JD and Burden RL, 2002. *Numerical Methods. Third Edition.* Brooks Cole.
16. G. Folland, 1995. *Introduction to Partial Differential Equations*, 1995.
17. Galon J, Costes A, Sanchez F, Kirilovsky A, Mlecnik B, Lagorce C, Tosolini M, Camus M, Berger A, Wind P, Zinzindohoue F, Bruneval P, Cugnenc P, Trajanoski Z, Fridman W, Page F, 2006. *Type, density, and location of immune cells within human colorectal tumors predict clinical outcome.* Science, 313:1960-1964. doi: 10.1126/science.1129139
18. Gilchrist D, Murphy D, Rashid B, 2012. *Generalisations of the strain-energy function of linear elasticity to model biological soft tissue.* International Journal of Non-Linear Mechanics, 47:268-72. doi:10.1016/j.ijnonlinmec.2011.06.004
19. Helmlinger G, Netti P, Lichtenbeld H, Melder R, Jain R, 1997. *Solid stress inhibits the growth of multicellular tumor spheroids.* Nature Biotechnology, 15:778-783. doi:10.1038/nbt0897-778
20. Jain RK, Martin JD, Stylianopoulos S, 2014. *The Role of Mechanical Forces in Tumor Growth and Therapy.* Annual Review of Biomedical Engineering, 16:321-346. doi:10.1146/annurev-bioeng-071813-105259
21. Jones A, Byrne H, Gibson J, Dold J, 2000. *A mathematical model of the stress induced during avascular tumor growth.* Journal of Mathematical Biology, 40:473-499.

doi:10.1007/s002850000033

22. Jones W, Chapman J, 2012. *Modeling Growth in Biological Materials.* SIAM Review, 54:52-118. doi:10.1137/080731785
23. Lax PD and Wendroff B, 1964. *Difference Schemes for Hyperbolic Equations with High Order of Accuracy.* Communications on Pure and Applied Mathematics, 17:381-398. doi:10.1002/cpa.3160170311
24. Liotta L, Kohn E, 2001. *The microenvironment of the tumourhost interface.* Nature, 411:375-379. doi:10.1038/35077241
25. Mascheroni P, Penta R, 2017. *The role of the microvascular network structure on diffusion and consumption of anti-cancer drugs.* International Journal for Numerical Methods in Biomedical Engineering. doi:10.1002/cnm.2857, 2017.
26. Mohme M, Maire C, Riecken K, Zapf S, Aranyossy T, Westphal M, Lamszus K, 2017. *Optical Barcoding for Single-Clone Tracking to Study Tumor Heterogeneity.* Molecular Therapy, 25:621-633. doi:10.1016/j.ymthe.2016.12.014
27. Montel F, Delaure M, Elgeti J, Vignjevic D, Cappello G, Prost J, 2012. *Isotropic stress reduces cell proliferation in tumor spheroids.* New Journal of Physics, 14:1-15. doi:10.1137/080731785
28. Ngwa M, Agyingi E, 2012. *Effect of an External Medium on Tumor Growth-induced Stress.* IAENG International Journal of Applied Mathematics, 42:229-236.
29. Pages F, Galon J, Dieu M, Tartour E, Sautes C, Fridman W, 2009. *Immune infiltration in human tumors: a prognostic factor that should not be ignored.* Oncogene, 29:10931102. doi:10.1038/onc.2009.416
30. Penta R, Ambrosi D, 2015. *The role of the microvascular tortuosity in tumor transport phenomena.* Journal of Theoretical Biology, 364:80-97. doi:10.1016/j.jtbi.2014.08.007
31. Penta R, Ambrosi D, Quarteroni A, 2015. *Multiscale homogenization for fluid and drug transport in vascularized malignant tissues.* Mathematical Models and Methods in Applied Sciences, 25:79108. doi:10.1142/S0218202515500037
32. Penta R, Ambrosi D, Shipley RJ, 2014. *Effective governing equations for poroelastic growing media.* The Quarterly Journal for Mechanics and Applied Mathematics, 67:6991. doi:10.1093/qjmam/hbt024
33. Penta R, Merodio J, 2017. *Homogenized modeling for vascularized poroelastic materials.* Meccanica. doi:10.1007/s11012-017-0625-1.
34. Ramírez-Torres A, Rodríguez-Ramos R, Merodio J, Bravo-Castillero J, Guinovart-Díaz R, Alfonso JCL, 2015. *Mathematical modeling of anisotropic avascular tumor growth.* Mechanics Research Communications, 69:8-14. doi:10.1016/j.mechrescom.2015.06.002
35. Ramírez-Torres A, Rodríguez-Ramos R, Merodio J, Penta R, Bravo-Castillero J, Guinovart-Díaz R, Sabina FJ, García-Reimbert C, Conci A, 2017. *The influence of anisotropic growth and geometry on the stress of solid tumors.* International Journal of Engineering Science, 119:40-49. doi:10.1016/j.ijengsci.2017.06.011
36. Ramírez-Torres A, Rodríguez-Ramos R, Sabina F J, García-Reimbert C, Penta R, Merodio J, Guinovart-Díaz R, Bravo-Castillero J, Conci A, Preziosi L, 2017. *The role of malignant tissue on the thermal distribution of cancerous breast.* Journal of Theoretical Biology, 426:152-161. doi:10.1016/j.jtbi.2017.05.031
37. Ricci SB, Cerchiari U, 2010. *Spontaneous regression of malignant tumors: Importance of the immune system and other factors (Review).* Oncology Letters, 1:941-945. doi:10.3892/ol.2010.176
38. Roose T, Netti PA, Munn LL, Boucher Y, Jain RK, 2003. *Solid stress generated by spheroid growth estimated using a linear poroelastic model.* Microvascular Research, 66:204-212.

doi:10.1016/S0026-2862(03)00057-8

39. Shi H, Farag A, 2005. *Validating linear elastic and linear viscoelastic models of lamb liver tissue using cone-beam CT.* International Congress Series, 1281:473-478. doi:10.1016/j.ics.2005.03.140
40. Shipley RJ, Rebecca J, Chapman SJ, 2010. *Multiscale modelling of fluid and drug transport in vascular tumours.* Bulletin of mathematical biology, 72:1464-1491. doi:10.1007/s11538-010-9504-9
41. Smith Z, 2014. *Fixed Point Methods in Nonlinear Analysis.* url:http://math.uchicago.edu/ may/REU2014/REUPapers/Smith,Z.pdf, last access 13 of June from 20174.
42. Stylianopoulos T, Martin JD, Chauhan VP, Jain SR, Diop-Frimpong B, Bardeesy N, Smith BL, Ferrone CR, Hornicek FJ, Boucher Y, Munn LL, Jain RK, 2012. *Causes, consequences, and remedies for growth-induced solid stress in murine and human tumors.* Proceedings of the National Academy of Sciences, 109:15101-15108. doi:10.1073/pnas.1213353109
43. Stylianopoulos T, Martin JD, Snuderl M, Mpekris F, Jain SR, Jain RK, 2013. *Coevolution of solid stress and interstitial fluid pressure in tumors during progression: implications for vascular collapse.* Cancer Research, 73:3833-41. doi:10.1158/0008-5472.CAN-12-4521
44. Sutherland R, 1988. *Cell and Environment Interactions in Tumor Microregions: The Multicell Spheroid Model.* Science, 240:177-184.
45. Unnikrishnan G, Unnikrishnan V, Reddy V, Lim C, 2010. *Review on the Constitutive Models of Tumor Tissue for Computational Analysis.* Applied Mechanics Reviews, 63:1-7. doi:10.1115/1.4002427
46. Tanaka M, Debinski W, Puri I, 2009. *Hybrid mathematical model of glioma progression.* Cell Proliferation, 42:637-646. doi:10.1111/j.1365-2184.2009.00631.x
47. Thomas JW, 1995. *Numerical Partial Differential Equations: Finite Difference Methods.* Springer.
48. Ward J, King J, 1997. *Mathematical modelling of avascular-tumour growth.* IMA Journal of Mathematics Applied in Medicine & Biology, 14:39-69.